Mobile Edge Computing via Wireless Power Transfer over Multiple Fading Blocks: An Optimal Stopping Approach

Qi Gu, Yiheng Jian, Gongpu Wang, *Member, IEEE*, Rongfei Fan, *Member, IEEE*, Hai Jiang, *Senior Member, IEEE*, and Zhangdui Zhong, *Senior Member, IEEE*

***Abstract*—To support wireless Internet of things (IoT) devices, this paper presents a new solution which combines wireless power transfer and mobile edge computing. Specifically, we consider one mobile device, which first harvests energy from radio frequency signals sent by a base station and then offloads all or part of its data to be processed to the base station. The process of energy harvesting and offloading span over multiple fading blocks. The target is to maximize the average amount of processed data in unit time. To achieve this target, we optimize the stopping rule for energy harvesting (i.e., when to stop energy harvesting and start offloading) and the number of fading blocks for data offloading. To solve the formulated problem optimally, we decompose it into two levels. In the lower level, the stopping rule for energy harvesting is optimized given a fixed number of fading blocks for offloading. The associated lower-level problem is solved optimally based on a series of special properties of the problem. In the upper level, the number of fading blocks for offloading is optimized. Efficiency of our work with fully offloading mode and partially offloading mode is shown by using simulation.**

***Index Terms*—Mobile edge computing (MEC), wireless power transfer, multiple fading blocks, optimal stopping.**

I. Introduction

The Internet of things (IoT) is a network of connected devices, which includes traditional Internet-connected devices, such as desktops, laptops, etc., as well as other devices that are not traditionally connected to the Internet, such as wireless sensors, automobiles, home appliances, etc. [1]–[4]. The connectivity among many categorizes of devices makes it easy to collect data from devices at distance and to control devices remotely, which enables people to interact with nearly every device anywhere. The functionality of IoT can facilitate the daily life of people, extend the reach of people in harsh environments, lower cost and enhance productivity in industry, etc. Thus, IoT has experienced rapid growth in recent years [5].

With the popularity of IoT, mobile devices need to process data (referred to as computation tasks) collected from other devices or from the environments. It may be difficult to locally compute the computation tasks at some mobile devices, e.g., devices with limited computation capacity and/or limited energy supply [6], [7]. To help the mobile devices to complete the computation tasks, mobile edge computing (MEC) can serve as a promising solution. In an MEC system, computation tasks of a mobile device with limited computation capability can be sent to a nearby base station (BS) with strong computation capability, and then the BS completes the computation tasks, and tells the mobile device the computation results [8]–[13].

On the other hand, it may also be hard for a mobile device in an IoT network to get stable energy supply. Thus, motivated by the idea of wireless power transfer (in which a receiver can harvest energy from radio frequency signals transmitted by a transmitter [14]), wireless-powered MEC is proposed and investigated in the literature [15]–[17]. In the system, a mobile device first harvests energy from the radio frequency signals sent by a nearby BS and then offloads all or part of its data to the BS for computing. The BS then sends back the computation results to the mobile device.

There are two open questions for wireless-powered MEC. 1) Most of the existing works [18]–[20] for data offloading in MEC assume that the whole data offloading process can be completed within a single fading block, and thus, during the whole data offloading process, the wireless channel gain does not change. However, the length of one fading block can be only at the scale of 2ms [21], while the maximal allowable delay of some applications, such as wearable devices, industrial Internet, smart farming, etc., can be at the scale of dozens of milliseconds or even longer [1], [5], [22]. Thus, it may need a number of fading blocks to complete the data offloading. For this case, existing offloading schemes that assume offloading over a single fading block do not work anymore, because it is difficult for a mobile device to predict the channel gains of forthcoming fading blocks for offloading. 2) In a wireless-powered MEC system, the energy harvesting and the data offloading processes alternate in time. A mobile device first harvests some energy, and then it stops harvesting energy and starts data offloading. It is unclear when it is optimal to stop the energy harvesting process and start the data offloading.

Manuscript received February 25, 2020; revised May 18, 2020; accepted June 22, 2020. This work was supported by the National Natural Science Foundation of China under Grant 61601025 and Grant 61771054. The review of this article was coordinated by Dr. F. Tang.

Qi Gu and Gongpu Wang are with the School of Computer and Information Technology, Beijing Jiaotong University, Beijing 100044, P. R. China (e-mail: 15112094@bjtu.edu.cn; gpwang@bjtu.edu.cn).

Yiheng Jian and Rongfei Fan are with the School of Information and Electronics, Beijing Institute of Technology, Beijing 100081, P. R. China (e-mail: 1120161318@bit.edu.cn; fanrongfei@bit.edu.cn).

Hai Jiang is with the Department of Electrical and Computer Engineering, University of Alberta, Edmonton, AB T6G 1H9, Canada (e-mail: hai1@ualberta.ca).

Zhangdui Zhong is with the State Key Laboratory of Rail Traffic Control and Safety, Beijing Jiaotong University, Beijing 100044, P. R. China (e-mail: zhdzhong@bjtu.edu.cn).

In this paper, we will focus on the above two open questions. Specifically, we consider one target mobile device in a multiple-user system. The mobile device is first wireless powered by a BS, and then offloads all or part of its computation tasks to the BS for computing. The energy harvesting process and the data offloading process span over multiple fading blocks. We target maximal data processing rate. To achieve this, we find out the optimal moment when the energy harvesting process should be stopped and the optimal number of fading blocks that the data offloading process should occupy.

The main contributions of our work are as follows.

- The formulated problem involves the optimization of a stopping rule and the number of fading blocks for data offloading. This problem is hard to solve. To find the solution of the formulated problem, we decompose the problem into two levels. In the lower level, the optimal stopping rule for energy harvesting is found for a given number of fading blocks in data offloading. In the upper level, the optimal number of fading blocks in data offloading is found.
- In the lower-level optimization problem, we find some interesting properties of the problem. Based on these properties and after some math manipulations, the optimal strategy is derived.
- In the upper level, we theoretically prove that the optimal number of fading blocks in data offloading should not be infinite. Based on this, the optimal number is found by a one-dimensional search.

The rest of this paper is organized as follows. In Section II, related literature is surveyed. Section III introduces the data offloading system over multiple fading blocks and formulates an optimization problem. Section IV and Section V discuss how to solve the lower-level problem and the upper-level problem, respectively. Numerical results are discussed in Section VI, and the conclusion is given in Section VII.

II. Related Works

The idea of powering IoT by MEC has been investigated in the literature [23], [24]. In [23], edge computing is proposed to assist IoT devices to run deep learning applications, such as feature extraction from voice or image. In [24], edge computing is utilized to perform channel assignment via deep learning methods so as to improve transmission quality in IoT delivery networks. Resource allocation for MEC IoT networks is investigated in [25]–[27]. In [25], network power consumption is minimized with a consideration of IoT devices' traffic and mobility. In [26], energy consumption of multiple IoT devices is minimized via adjusting the bandwidth allocated to every IoT device. In [27], the number of activated edge computing BSs is minimized with a consideration of multiple IoT devices' spacial distribution and mobility. In [28], a scalable deployment solution is given for a massive number of IoT devices in 6G wireless networks by using a machine learning approach.

The works mentioned above study MEC powered IoT networks from the network layer. Wireless fading is not considered. In the following, we survey works on MEC powered IoT networks over wireless fading channels.

It is considered in [18] that a computation task of a mobile device can be computed jointly by the mobile device and a BS. The ratio of data for offloading and the wireless transmission power level are optimized. In [19], it is assumed that the CPU state of an edge-computing BS switches between "busy" and "idle" and the BS's CPU-idling profile (i.e., the time windows when the BS's CPU is idle in the future) is known. The most energy-saving strategy is designed by optimizing the offloaded data amount. The authors in [20] investigate the case when both the mobile device and the BS are equipped with multiple antennas.

It is assumed in [18]–[20] that the whole data offloading process can be completed within a single fading block, and thus, during the whole data offloading process, the wireless channel gain does not change. Considering that the tolerable delay in many IoT applications [1], [5], [22] is much larger than a fading block duration (which is at scale of 2 ms [21]), data offloading should experience varying wireless channel gains over multiple fading blocks, and thus, the methods in [18]–[20] do not work anymore.

The work in [29] considers that data offloading occurs within a number of fading blocks. A mobile device either performs all the computation itself, or offloads all its data to a BS, whichever consumes less energy of the mobile device. If offloading happens, the most energy efficient strategy is designed by optimally distributing data over multiple fading blocks, based on a two-state channel modeling. The work in [30] also investigates the case when data offloading occurs within a number of fading blocks, by using a general channel modeling.

The aforementioned works consider that the mobile devices have constant power supply. To the best of our knowledge, the works in [16], [17] are the only technical research efforts in the literature that investigate wireless-powered MEC. The work in [16] considers data offloading over a single fading block, with a BS, a near mobile device, and a far mobile device. The two mobile devices first harvest energy from the BS, and then offload their data to the BS. The near mobile device sends its data to the BS, and also provides relaying service for the far mobile device's data offloading. The work in [17] considers offloading of a mobile device to a BS over a number of fading blocks, referred to as *offloading fading blocks* here. At the beginning of the offloading process, the mobile device is assumed to know the channel state information (CSI) of all future offloading fading blocks. Two working modes are considered: fully offloading and fully local computing. For fully offloading mode, in every fading block, the mobile device first gets charged by RF signals from the BS, and then offloads its data to the BS. The fraction of time for energy harvesting in every fading block and the amount of data to be offloaded in every fading block are optimized so as to maximize the total amount of saved energy. For fully local computing mode, an energy-efficient strategy is designed, which decides the amount of data for processing in each fading block.

In this paper, we investigate the problem of wireless-powered MEC over multiple fading blocks. The major differ-

TABLE I: Notations used

Symbols	Description
c_0	number of required CPU cycles for computing a data nat
C	energy capacity of the battery
D_E	amount of offloaded data nats in partial offloading
D_L	amount of locally computed data nats in partial offloading
$D_f(y, M)$	the maximal amount of data nats that can be processed in the M offloading fading blocks at the mobile device with energy level y in fully offloading mode
$D_p(y, M)$	the maximal amount of data nats that can be processed in the M offloading fading blocks at the mobile device with energy level y in partial offloading mode
$e(d, g)$	the energy consumption within the fading block with channel gain being g for offloading d nats
$E(N)$	the total available energy in the battery of mobile device by the end of EH fading block N
$f(x)$	channel gain distribution between BS and mobile device
g_n	the channel gain from mobile device to BS in offloading fading block n
$\boldsymbol{g}$	$(g_M, g_{M-1}, ..., g_1)^T$
h_n	the channel gain from BS to mobile device in EH fading block n
$h_{1\to n}$	$\{h_1, h_2, ..., h_n\}$
$\mathcal{I}$	the set of integers
$J_m(d)$	minimum energy amount that the mobile device expects to consume for offloading d data nats when the device is at the beginning of offloading fading block m but has not measured the channel gain g_m yet
k	parameter related to mobile device's CPU features
M	the number of fading blocks for data offloading
N	the number of fading blocks for EH
P_E	transmit power of BS
η	energy conversion efficiency
$\Lambda_M(D)$	the minimum energy needed to process D data nats in M offloading fading blocks under partially offloading mode
σ^2	noise power spectrum density
τ	length of one fading block
$\tau_{N,M}$	the total time duration for N EH fading blocks and M offloading fading blocks

ence between our work and [17] lies in the system assumption. The work in [17] assumes that the mobile device knows CSI of future fading blocks in the data offloading process. We assume that the mobile device knows only CSI of its current fading block, while the CSI of future fading blocks is assumed to be unknown.

III. System Model and Problem Formulation

In this section, system model will be introduced, including the model for energy harvesting, computing and data offloading. Then our optimization problem will be formulated. Important notations used in this work are given in Table I.

A. System Model

Consider an MEC system, in which there are one BS and multiple mobile devices. Every mobile device always has data (i.e., computation tasks) to process, and is allocated with one channel which has a bandwidth of w. On each channel, the associated mobile device is charged by the BS via wireless power transfer (WPT) technique, and then offloads all or part of its data to the BS for computing, in order to save its energy consumption. After the BS finishes computing the offloaded data, it tells the mobile device the computation results. When the mobile device offloads part of its data, it performs local computing for the rest of its data. In this research, we consider only a target channel and the associated mobile device, as the derived solution for the associated mobile device can also be applied by other mobile devices. Fig. 1 shows the BS and the mobile device on the target channel.

The wireless charging (i.e., energy harvesting) and data offloading alternate in time. In one round of energy harvesting and data offloading, the mobile device first harvests energy from zero to some level, and then stops harvesting energy and uses up all the available energy to offload data and/or execute local computing. This charging-offloading process is repeated round by round. In this research, we investigate the optimal performance that can be achieved in a round.

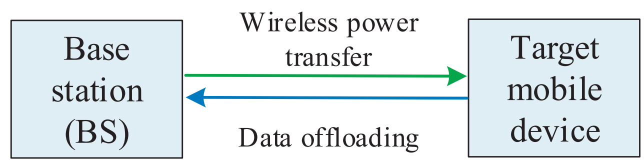

Fig. 1: Illustration of our system with a BS and the target mobile device.

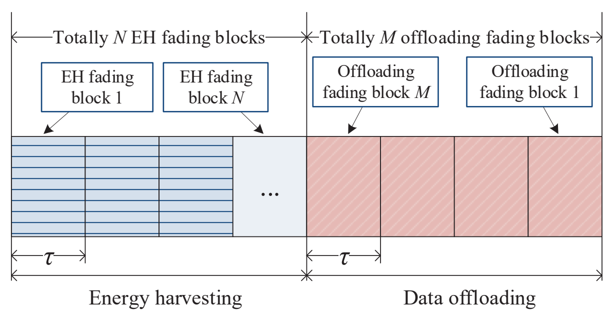

Fig. 2: One round of energy harvesting and data offloading processes.

In the system, the channel gain between the BS and the mobile device is block-faded, i.e., the channel gain keeps stable in one fading block and changes randomly from fading block to fading block. The duration of each fading block is τ. The channel gain of the fading blocks are independent and identically distributed, which is subject to the distribution function $f(x)$ and upper bounded by h_u, i.e., we have $f(x) = 0$ for $x \geq h_\text{u}$. Both energy harvesting and data offloading may span over multiple fading blocks.

In one round of energy harvesting and data offloading, denote N and M as the number of fading blocks in energy harvesting and data offloading, respectively, as shown in Fig. 2. We call the N fading blocks for energy harvesting (EH) as *EH fading blocks*, indexed as EH fading block 1, EH fading block $2, ...,$ EH fading block N, with channel gains (from the BS to the mobile device) denoted as $h_1, h_2, ..., h_N$, respectively. We call the M fading blocks for data offloading as *offloading fading blocks*, indexed as offloading fading block M, offloading fading block $M-1, ...,$ offloading fading block

1, with channel gains (from the mobile device to the BS) denoted as $g_M, g_{M-1}, ..., g_1$, respectively. In other words, for presentation simplicity, the beginning fading block in data offloading is called offloading fading block M, while the ending fading block in data offloading is called offloading fading block 1.

Energy harvesting is performed over multiple fading blocks. At the beginning of EH fading block 1, the energy level of the mobile device is 0, and then the mobile device starts to harvest energy. Denote the transmit power of the BS as P_E, and the energy conversion efficiency of the energy harvester at the mobile device as η. Then the harvested energy in EH fading block $n (n \in \{1, 2, ..., N\})$ is $\eta P_E \tau h_n$. Assume the maximal energy capacity of the battery of the energy harvester is C. By the end of EH fading block N, the total available energy in the battery of the mobile device can be written as

$$E(N) = \min\left\{\eta P_E \tau \sum_{n=1}^{N} h_n, C\right\}. \tag{1}$$

For data offloading, two modes are considered.

- Fully Offloading Mode: The mobile device offloads all its data to be processed at the BS.
- Partially Offloading Mode: The mobile device offloads part of its data to be processed at the BS, and computes the rest of its data locally.

Here we assume that computing time at the BS and the downlink transmission time of the computation results are negligible, due to the following reasons. 1) As indicated in [10], [11], the computing capability of the BS is usually high, and thus, the computation time at the BS is small; and after the BS finishes the computing, the amount of computation results to be sent back to the mobile device is usually of small size. 2) In our system, the bottleneck resources are the mobile device's energy and uplink transmission capacity, and thus, our focus is to efficiently utilize the two bottleneck resources. In our system, the mobile device has multiple rounds of operations, and in each round, the mobile device first harvests energy and then offloads its data to the BS. Consider Round j. After the mobile device finishes offloading data to the BS, the BS starts to compute the received data, while the mobile device can start Round $(j+1)$ immediately (i.e., the mobile device does not need to wait until the computation results are sent back). So the computing at the BS and the mobile device's operations in Round $(j+1)$ *can happen in parallel*. For example, in Round $(j+1)$'s EH fading blocks (in which the mobile device harvests energy), the BS can compute the data it received in Round j, and then send back computation results by using a downlink channel. In other words, the BS's computing and computation result feedback do not consume the system's bottleneck resources (the mobile device's energy and uplink transmission capacity). Thus, the BS's computing of data received in Round j and the subsequent computation result feedback can happen in Round $(j+1)$ or even beyond Round $(j+1)$.

1) Fully Offloading Mode: In this mode, all available energy is used for offloading.

By the end of EH fading block N, the available energy in total for the mobile device is $E(N)$ given in (1). For the fully offloading mode, denote $D_{\mathrm{f}}(E(N), M)$ as the maximal amount of data nats that can be processed (i.e., offloaded) in the M offloading fading blocks at the mobile device with energy level $E(N)$. Here subscript 'f' stands for fully offloading mode.

In an offloading fading block, say offloading fading block m ($m \in \{1, 2, ..., M\}$), if the channel gain is g_m, then the amount of data nats that can be offloaded in the fading block is expressed as [21]

$$d_m = w\tau \ln\left(1 + \frac{p_m g_m}{w\sigma^2}\right), \tag{2}$$

where p_m is transmit power of the mobile device in offloading fading block m, and σ^2 is noise power spectrum density. Looking into (2), transmit power p_m can be expressed as a function of d_m and g_m as

$$p_m\left(d_m, g_m\right) = \frac{\left(e^{\frac{d_m}{w\tau}} - 1\right) w\sigma^2}{g_m}. \tag{3}$$

Hence the energy consumption within the offloading fading block for offloading d_m data nats is given by

$$\begin{aligned} e\left(d_m, g_m\right) &= p_m\left(d_m, g_m\right)\tau \\ &= \frac{\left(e^{\frac{d_m}{w\tau}} - 1\right) w\sigma^2\tau}{g_m}. \end{aligned} \tag{4}$$

Next we try to characterize $D_{\mathrm{f}}(E(N), M)$. For this purpose, we denote $J_m(d)$ as follows. Consider that the mobile device is at the beginning of offloading fading block m but has not measured the channel gain g_m yet. For the mobile device to offload d data nats within the remaining offloading fading blocks (i.e., from the current offloading fading block until offloading fading block 1), denote $J_m(d)$ as the minimum amount of energy that the mobile device expects to consume. It is straightforward to see that $D_{\mathrm{f}}(E(N), M) = J_M^{-1}(E(N)\varepsilon)$, where $\varepsilon \in (0, 1)$ is the efficiency of the amplifier at the transmitter of the mobile device, and $J_M^{-1}(\cdot)$ is the inverse function of $J_M(\cdot)$. Thus, to characterize $D_{\mathrm{f}}(E(N), M)$, we should characterize $J_M(\cdot)$, by following a similar procedure to that in [30].

When the mobile device is at the beginning of offloading fading block m and has measured the channel gain g_m, denote $Q_m(d, g_m)$ as the minimum amount of energy that the mobile device expects to consume for offloading d data nats within the remaining offloading fading blocks (i.e., from the current offloading fading block until offloading fading block 1). Then we have

$$J_M(d) = \int_0^\infty Q_M(d, g_M) f(g_M) dg_M.$$

For energy consumption $Q_M(d, g_M)$, it contains two portions: the energy used in offloading fading block M, and the energy used in subsequent offloading fading blocks (i.e., offloading fading blocks $M-1, M-2, ..., 2, 1$). Denote d' as the offloaded data amount in offloading fading block M. Then the energy used in offloading fading block M can be expressed as $e(d', g_M)$, and the energy used in subsequent offloading fading blocks can be expressed as $J_{M-1}(d-d')$. As $Q_M(d, g_M)$ is the *minimum expected* energy consumption, we have

$$Q_M(d, g_M) = \min_{0\leq d'\leq d} \left\{ e(d', g_M) + J_{M-1}(d-d') \right\}.$$

In the above expression, we need to characterize $J_{M-1}(\cdot)$. We can follow the same procedure as we treat $J_M(\cdot)$. This procedure is repeated until offloading fading block 1.

To summarize the procedure from offloading fading block M until offloading fading block 1, we have

$$J_m(d) = \int_0^{\infty} Q_m(d, g_m) f(g_m) dg_m, \quad \forall m = M, M-1, ..., 2, 1, \tag{5}$$

$$Q_m(d, g_m) = \begin{cases} \min_{0\leq d'\leq d} \left\{ e(d', g_m) + J_{m-1}(d-d') \right\}, & \forall m = M, M-1, ..., 3, 2 \\ e(d, g_1), & m = 1. \end{cases} \tag{6}$$

It can be seen that the recursive procedure shown in (5) and (6) is actually a dynamic programming procedure [29]–[31]. By using dynamic programming approaches, $J_M(\cdot)$ can be characterized. And as aforementioned, we have $D_{\rm f}(E(N), M) = J_M^{-1}(E(N)\varepsilon)$.

2) Partially Offloading Mode: In this mode, the available energy at the mobile device is used for both offloading and local computing. Recall that by the end of EH fading block N, the available energy in total for the mobile device is $E(N)$ given in (1). Denote $D_{\rm p}(E(N), M)$ as the maximal amount of data nats that can be offloaded and locally computed in the M offloading fading blocks at the mobile device with energy level $E(N)$. Here subscript 'p' stands for partially offloading mode.

To characterize $D_{\rm p}(E(N), M)$, we try to find out the minimum energy needed to process (i.e., offload and locally compute) D data nats in M offloading fading blocks, denoted as $\Lambda_M(D)$. We can see that

$$D_{\rm p}(E(N), M) = \Lambda_M^{-1}(E(N)\varepsilon), \tag{7}$$

where $\Lambda_M^{-1}(\cdot)$ is the inverse function of $\Lambda_M(\cdot)$.

Now we try to find out $\Lambda_M(D)$. For the D data nats, denote $D_{\rm L}$ and $D_{\rm E}$ as the amount of data nats to be locally computed at the mobile device and to be offloaded to the BS, respectively. Here subscript 'L' and 'E' stand for "local" and "external", respectively. Then we have

$$D = D_{\rm L} + D_{\rm E}. \tag{8}$$

For the mobile device to locally compute $D_{\rm L}$ data nats, the consumed energy can be written as [18]

$$E_{\rm L}(D_{\rm L}, T) = \frac{k c_0^3 D_{\rm L}^3}{T^2}, \tag{9}$$

where k is a parameter related to the features of the mobile device's CPU, c_0 is the number of required CPU cycles for computing a data nat, and T is the computation time.

Thus, $\Lambda_M(D)$ can be given as

$$\begin{aligned} \Lambda_M(D) = \quad & \min_{D_{\rm E}} \quad E_{\rm L}(D - D_{\rm E}, M\tau) + J_M(D_{\rm E}) \\ & \text{s.t.} \quad\quad 0 \leq D_{\rm E} \leq D. \end{aligned} \tag{10}$$

By using (10), $\Lambda_M(D)$ can be found off-line via a one-dimensional exhaustive search. With $\Lambda_M(D)$, $D_{\rm p}(E(N), M)$ can be expressed as in (7).

B. Problem Formulation

When the mobile device stops energy harvesting at the end of EH fading block N, the amount of data nats that can be processed is $D_i(E(N), M)$ for $i \in \{\rm f, p\}$, and the total time duration for energy harvesting and offloading is

$$\tau_{N,M} = N\tau + M\tau. \tag{11}$$

Here N is called the *stopping time*, which is a random variable with values in $\{1, 2, ...\}$. In optimal stopping theory, N is also called *stopping rule*.

At an EH fading block (say EH fading block l), after the energy is harvested in the fading block, the mobile device needs to decide whether to continue energy harvesting or to stop energy harvesting. If the mobile device decides to stop energy harvesting (i.e., $N = l$), then it processes (i.e., offloads and/or locally computes) its data in the subsequent M offloading fading blocks. If the mobile device decides to continue energy harvesting, it harvests energy in the next fading block and makes a decision again (i.e., to continue or to stop energy harvesting).

When the stopping rule N is applied repeatedly for K times, there are K independent and identically distributed stopping time moments $\{N_1, N_2, ..., N_K\}$. Thus, average processed data amount in unit time with K rounds (each round containing one energy harvesting process and one offloading process) is given as $\left(\sum_{k=1}^K D_i(E(N_k), M)\right) / \left(\sum_{k=1}^K \tau_{N_k,M}\right)$ for $i \in \{\rm f, p\}$. When K goes to infinity, the average processed data amount in unit time can be written as

$$\lim_{K\to\infty} \frac{\sum_{k=1}^K D_i(E(N_k), M)}{\sum_{k=1}^K \tau_{N_k,M}} = \frac{\mathbb{E}[D_i(E(N), M)]}{\mathbb{E}[\tau_{N,M}]} \tag{12}$$

almost surely. Here $\mathbb{E}[\cdot]$ means expectation. Our research goal is to design the optimal stopping rule N and select M so as to maximize the average processed data amount in unit time. Specifically, the optimization problem is given as follows.

Problem 1:

$$\max_{N\in\mathcal{Q}_M, M\in\mathcal{I}, M\geq 1} \frac{\mathbb{E}[D_i(E(N), M)]}{\mathbb{E}[\tau_{N,M}]} \tag{13}$$

where $\mathcal{Q}_M \triangleq \{N | N \geq 1, \mathbb{E}[\tau_{N,M}] < \infty\}$ is the set of all stopping rules, $i \in \{\rm f, p\}$, and $\mathcal{I}$ is the set of integers.

To solve Problem 1, we decompose it into two levels. Specifically, in the lower-level problem, we find the optimal stopping rule for a given M value. Accordingly, the lower-level problem is

Problem 2:

$$R(M) \triangleq \max_{N\in\mathcal{Q}_M} \frac{\mathbb{E}[D_i(E(N), M)]}{\mathbb{E}[\tau_{N,M}]}. \tag{14}$$

In the upper-level problem, we try to find the optimal value of M. Accordingly, the upper-level problem is

Problem 3:

$$\max_{M\in\mathcal{I},M\geq 1} R(M). \tag{15}$$

Next, we first solve the lower-level problem (Problem 2) in Section IV. Then based on the optimal solution of Problem 2, we solve the higher-level problem (Problem 3) in Section V.

IV. Solution of the Lower-Level Problem: Problem 2

To solve Problem 2 optimally, some features of functions $D_{\mathrm{f}}(y,m)$ and $D_{\mathrm{p}}(y,m)$ are characterized first in the following lemmas (the proofs are given in Appendix A and Appendix B).

Lemma 1: $D_{\mathrm{f}}(y,m)$ is an increasing and concave function with respect to y.

Lemma 2: $D_{\mathrm{p}}(y,m)$ is an increasing and concave function with respect to y.

According to the optimal stopping theory [32], solving Problem 2 is equivalent to finding λ^* such that $V_i^*(\lambda^*,M)=0$, where $V_i^*(\lambda,M)$ is defined as

Problem 4:

$$V_i^*(\lambda,M)=\sup_{N\in\mathcal{Q}_M}\mathbb{E}[D_i(E(N),M)-\lambda\tau_{N,M}],\ \lambda>0. \tag{16}$$

For given λ, to get the optimal solution of Problem 4, the following lemma can be expected.

Lemma 3: The optimal stopping rule for Problem 4 is the myopic stopping rule, i.e., define $z_{i,n}=D_i(E(n),M)-\lambda\tau_{n,M}$ for $i\in\{\mathrm{f},\mathrm{p}\}$, the optimal stopping time is given as

$$N_i^*(\lambda,M)=\min\{n: z_{i,n}\geq\mathbb{E}[z_{i,n+1}|h_{1\to n}]\} \tag{17}$$

where $h_{1\to n}=\{h_1,h_2,...,h_n\}$.

Proof: According to [32], for Problem 4, the myopic rule is optimal if three conditions can all be met:

(i) We can express $z_{i,n}$ in the form of $z_{i,n}=v_{i,n}-u_{i,n}$. Here $\mathbb{E}[\sup_n|v_{i,n}|]$ is less than infinity, and the nonnegative component $u_{i,n}$ is nondecreasing almost surely;

(ii) $\lim\limits_{n\to\infty} z_{i,n}=z_{i,\infty}$ almost surely;

(iii) Problem 4 is a monotone problem.

Firstly, $z_{i,n}=D_i(E(n),M)-\lambda\tau_{n,M}=D_i(E(n),M)-\lambda(n\tau+M\tau)$, where $\lambda(n\tau+M\tau)$ is nonnegative and nondecreasing with respect to n and $\mathbb{E}[\sup\limits_n|D_i(E(n),M)|]\leq\mathbb{E}[D_i(C,M)]<\infty$, where C is the maximal energy capacity of the mobile device's battery. Thus Condition (i) is satisfied.

Secondly, $z_{i,n}=D_i(E(n),M)-\lambda\tau_{n,M}$. When $n\to\infty$, $\tau_{n,M}\to\infty$, and $E(n)\leq C<\infty$, thus we have $\limsup\limits_{n\to\infty} z_{i,n}\to-\infty$. Due to the fact that $\liminf\limits_{n\to\infty} z_{i,n}\leq\limsup\limits_{n\to\infty} z_{i,n}=-\infty$, we have

$$\lim_{n\to\infty} z_{i,n}=\liminf_{n\to\infty} z_{i,n}=\limsup_{n\to\infty} z_{i,n}=-\infty. \tag{18}$$

Hence Condition (ii) is satisfied.

Finally, we try to prove Condition (iii). Define $\mathcal{A}_{i,n}\triangleq\{z_{i,n}\geq\mathbb{E}[z_{i,n+1}|h_{1\to n}]\}$. A monotone problem means that $\mathcal{A}_{i,0}\subseteq\mathcal{A}_{i,1}\subseteq\ldots\subseteq\mathcal{A}_{i,n}$. Namely, if there is

$$z_{i,n}\geq\mathbb{E}[z_{i,n+1}|h_{1\to n}], \tag{19}$$

then the following inequality always holds:

$$z_{i,n+1}\geq\mathbb{E}[z_{i,n+2}|h_{1\to(n+1)}]. \tag{20}$$

For $z_{i,n}$, we have

$$\begin{aligned} z_{i,n}=D_i\left(\min\left\{C,\eta P_E\tau(h_1+h_2+...+h_n)\right\},M\right)\\ -\lambda(n\tau+M\tau). \end{aligned} \tag{21}$$

Substitute (21) into (19) and (20) respectively, (19) is equivalent to

$$D_i\left(\min\left\{C,B_n\right\},M\right)\geq\mathbb{E}\left[D_i\left(\min\left\{C,B_{n+1}\right\},M\right)\right]-\lambda\tau, \tag{22}$$

and (20) is equivalent to

$$D_i\left(\min\{C,B_{n+1}\},M\right)\geq\mathbb{E}\left[D_i\left(\min\{C,B_{n+2}\},M\right)\right]-\lambda\tau \tag{23}$$

where $B_n=\eta P_E\tau(h_1+h_2+...+h_n)$. It is straightforward to see that

$$B_n\leq B_{n+1}. \tag{24}$$

Thus, we only need to prove that when (22) holds, (23) also holds.

To complete this proof, three possible cases need to be considered, as follows.

(a) $C\leq B_n\leq B_{n+1}$. In this case, $B_{n+2}\geq B_{n+1}\geq C$, thus $\min\{C,B_{n+1}\}=\min\{C,B_{n+2}\}=C$, which indicates the holding of (23) naturally.

(b) $B_n\leq C\leq B_{n+1}$. In this case, the same proof for the case in (a) also works.

(c) $B_n\leq B_{n+1}<C$. In this case, we need to prove that

$$D_i(B_n,M)\geq\mathbb{E}[D_i(\min\{C,B_n+\eta P_E\tau h_{n+1}\},M)]-\lambda\tau \tag{25}$$

can lead to

$$\begin{aligned} D_i(B_{n+1},M)\geq&\mathbb{E}[D_i(\min(C,B_{n+1}+\eta P_E\tau h_{n+2}),M)]\\ &-\lambda\tau. \end{aligned} \tag{26}$$

This can be proved by showing that

$$\begin{aligned} &\mathbb{E}[D_i(\min\{C,x+\eta P_E\tau h_n\},M)]-D_i(x,M)\\ &=\int D_i(\min\{C,x+\eta P_E\tau h\},M)f(h)dh\\ &\quad-\int D_i(x,M)f(h)dh \end{aligned} \tag{27}$$

is a decreasing function with respect to x when $x<C$, which is equivalent to showing that

$$D_i(\min\{C,x+\eta P_E\tau h\},M)-D_i(x,M) \tag{28}$$

is a decreasing function with respect to x.

We consider $x_1\leq x_2<C$:

- When $x_2+\eta P_E\tau h<C$: Define the first-order derivative function of $D_i(x,M)$ with x as $G_i(x,M)$.

Since $D_i(x, M)$ is an increasing and concave function according to Lemma 1 and Lemma 2, $G_i(x, M)$ is a decreasing function with respect to x. Hence we have

$$G_i(x_1 + \Delta, M) \geq G_i(x_2 + \Delta, M), \ \ \Delta \in [0, \eta P_E \tau h] \tag{29}$$

$$\Rightarrow \int_{x_1}^{x_1 + \eta P_E \tau h} G_i(x, M) dx \geq \int_{x_2}^{x_2 + \eta P_E \tau h} G_i(x, M) dx \tag{30}$$

$$\Rightarrow D_i(x_1 + \eta P_E \tau h, M) - D_i(x_1, M) \geq D_i(x_2 + \eta P_E \tau h, M) - D_i(x_2, M), \tag{31}$$

which proves that the expression in (28) decreases with respect to x.

- When $x_2 + \eta P_E \tau h \geq C$: We have $D_i(x_2 + \eta P_E \tau h, M) \geq D_i(C, M)$. Combining (31), we have

$$D_i(x_1 + \eta P_E \tau h, M) - D_i(x_1, M) \geq D_i(C, M) - D_i(x_2, M), \tag{32}$$

which proves that the expression in (28) decreases with respect to x.

Therefore, the inequality (26) is proved.

To this end, we can state that (23) holds, which indicates that Problem 4 is monotone.

This completes the proof. ∎

Lemma 3 offers the following insight. To find out the optimal stopping rule that achieves the maximal utility of Problem 4 for a given λ, the mobile device only needs to do an easy on-line computing. At every EH fading block, say EH fading block n, the mobile device should compare $z_{i,n}$ with $\mathbb{E}\left[z_{i,n+1} | h_{1 \to n}\right]$. If $z_{i,n}$ is larger, then the mobile device stops energy harvesting and starts data offloading; otherwise, the mobile device proceeds to the next fading block and repeats the procedure again.

To find the optimal solution of Problem 2, i.e., to find the λ^* such that $V_i^*(\lambda^*, M) = 0$, a bisection search method can be utilized. In the bisection search, we need to know the values of $V_i^*(\lambda, M)$ for some particular λ values. This can be done off-line by using Monte Carlo method with the help of Lemma 3, as shown in Algorithm 1.

Algorithm 1 Calculation of $V_i^*(\lambda, M)$ for a given λ value.

Suppose the number of Monte Carlo simulation runs is Q and set $q = 1$.
while $q < Q$ **do**
  Set $n = 1$. Randomly generate h_n according to the distribution $f(h)$. Evaluate $\mathbb{E}\left[z_{i,n+1} | h_{1 \to n}\right]$.
  while $z_{i,n} < \mathbb{E}\left[z_{i,n+1} | h_{1 \to n}\right]$ **do**
    Randomly generate h_{n+1} according to the distribution $f(h)$.
    $n = n + 1$.
  Record the present $z_{i,n}$.
  $q = q + 1$.
$V_i^*(\lambda, M)$ is evaluated as the statistical mean of all the recorded $z_{i,n}$.

To this end, how to find the optimal stopping rule N for Problem 2 has been presented. As a summary, the computational complexity to solve Problem 2 is composed of the following three components: 1) Bisection search of λ^* such that $V_i^*(\lambda^*, M) = 0$ for $i \in \{f, p\}$; 2) The calculation of Algorithm 1 for every λ. 3) The evaluation of function $D_i(E(N), M)$ for $i \in \{f, p\}$ in expression of $z_{i,n}$ when running Algorithm 1.

- For the computational complexity of $D_i(E(N), M)$ for $i \in \{f, p\}$, we use dynamic programming, whose computational complexity is in the order of $O(e^M)$.
- For the computational complexity of Algorithm 1, we have Q Monte Carlo simulation runs. In each simulation run, the complexity is proportional to the number of n values searched. However, it is hard to predict when to stop searching (i.e., when $z_{i,n} \geq \mathbb{E}\left[z_{i,n+1} | h_{1 \to n}\right]$) since the channel gains $h_1, h_2, ..., h_n$ are all random. Even with the distribution function of $h_1, h_2, ..., h_n$, the distribution of stopping time is also hard to characterize since we have no closed-form expression of $D_i(x, M)$ for $i \in \{f, p\}$ ($D_i(x, M)$ is a component in $z_{i,n}$ expression). Therefore, it is hard to give an analytical expression for the complexity of Algorithm 1. In Section VI, we plot the average stopping time versus the mean of channel gain in Fig. 10. This figure would be helpful for evaluating the complexity of Algorithm 1.
- For the bisection search of λ^*, suppose λ^* is searched between $\lambda_{\min}$ and $\lambda_{\max}$, and the error tolerance of λ^* is δ. Then the computational complexity of the bisection search is $O(\log\left(\frac{\lambda_{\max} - \lambda_{\min}}{\delta}\right))$.

Note that the above three computation components can all be done off-line. In a real application, to achieve the maximal utility of Problem 2 for a given M, the mobile device only needs to do a simple on-line computing enlightened by Lemma 3. Specifically, with λ^* calculated off-line, at every EH fading block, say EH fading block n, the mobile device stops when $z_{i,n} \geq \mathbb{E}\left[z_{i,n+1} | h_{1 \to n}\right]$ and proceeds to the next EH fading block otherwise. In other words, a simple comparison is needed for each EH fading block. The online computation complexity is $O(1)$.

V. Solution of the Upper-Level Problem: Problem 3

For Problem 3, we have some analytical results as follows (proofs are given in Appendix C, Appendix D, and Appendix E).

Lemma 4: With d fixed, $J_m(d)$ is monotonically decreasing with m.

Lemma 5: With d fixed, $\Lambda_m(d)$ is monotonically decreasing with m.

Lemma 6: With the stopping time N fixed, both the function $\mathbb{E}[D_i(E(N), M)]$ and the function $\mathbb{E}[\tau_{N,M}]$ are monotonically increasing functions with M for $i \in \{\text{f}, \text{p}\}$.

According to Lemma 6, both the numerator and the denominator of Problem 1's objective function are monotonically increasing with M. Hence it is hard to say whether the optimal solution of Problem 3 is finite or infinite. The following lemma addresses this issue.

Lemma 7: The optimal solution of Problem 3 is finite.

Proof: To prove this claim, it is sufficient to show that the optimal solution of M does not happen at $M=\infty$, which will hold if

$$\lim_{M\to\infty}\frac{\mathbb{E}[D_i(E(N),M)]}{\mathbb{E}[\tau_{N,M}]}=0 \tag{33}$$

for any given stopping time N. With stopping time N given, it can be seen that $\mathbb{E}\left[\tau_{N,M}\right]$ increases with M linearly. Thus to prove the claim in this lemma, we only need to show that $\mathbb{E}\left[D_i(E(n),M)\right]$ grows with M sublinearly as M goes to infinity by L'Hospital's rule, which is equivalent to the following condition

$$\lim_{M\to\infty}\frac{D_i(E(n),M)}{M}=0 \tag{34}$$

for $i\in\{\mathrm{f},\mathrm{p}\}$.

Define notation $\boldsymbol{g}=(g_M,g_{M-1},...,g_1)^T$ with $(\cdot)^T$ representing transpose operation, and denote $f(\boldsymbol{g})$ as the joint probability density function (PDF) of $\boldsymbol{g}$, i.e., $f(\boldsymbol{g})=\prod_{m=1}^M f(g_m)$.

For $i=\mathrm{f}$, define

$$\begin{aligned} E_{\mathrm{f}}(d,\boldsymbol{g})\triangleq \min_{\{d_m|m\in\{1,2,...,M\}\}} \quad & \sum_{m=1}^{M} e(d_m,g_m)\\ \text{s.t.} \quad & \sum_{m=1}^{M} d_m=d,\\ & d_m\geq 0,\forall m\in\{1,2,...,M\}. \end{aligned} \tag{35}$$

Also define $E_{\mathrm{f}}(d)\triangleq\int E_{\mathrm{f}}(d,\boldsymbol{g})f(\boldsymbol{g})d\boldsymbol{g}$. It can be seen that $E_{\mathrm{f}}(d)$ is calculated by assuming that $g_1,g_2,...,g_M$ are known in advance at the beginning of the data offloading phase. From (5), it can be seen that $J_M(d)$ is calculated by assuming that only channel gain information of the current offloading fading block is known. Thus, it is apparent that we have

$$J_M(d)>E_{\mathrm{f}}(d). \tag{36}$$

Then by following the similar proof method in Lemma 6, it can be inferred that

$$D_{\mathrm{f}}(E(n),M)=J_M^{-1}(E(n)\varepsilon)<E_{\mathrm{f}}^{-1}(E(n)\varepsilon) \tag{37}$$

where $E_{\mathrm{f}}^{-1}(\cdot)$ is the inverse function of $E_{\mathrm{f}}(\cdot)$.

For the function $e(d_m,g_m)$ in (35), it can be derived that

$$e(d_m,g_m)\geq\frac{\sigma^2}{6w^2\tau^2 g_m}d_m^3, \tag{38}$$

because the first order derivative of $\left(e(d_m,g_m)-\frac{\sigma^2}{6w^2\tau^2 g_m}d_m^3\right)$ with respect to d_m is larger than zero. Define $E_{\mathrm{f,\,lb}}(d,\boldsymbol{g})$ as

$$\begin{aligned} E_{\mathrm{f,\,lb}}(d,\boldsymbol{g})\triangleq \min_{\{d_m|m\in\{1,2,...,M\}\}} \quad & \sum_{m=1}^{M}\frac{\sigma^2}{6w^2\tau^2 g_m}d_m^3\\ \text{s.t.} \quad & \sum_{m=1}^{M} d_m=d, && \text{(39a)}\\ & d_m\geq 0,\forall m\in\{1,2,...,M\} && \text{(39b)} \end{aligned}$$

in which subscript 'lb' stands for "lower bound". From (38), we know that $E_{\mathrm{f,\,lb}}(d,\boldsymbol{g})$ is a lower bound of $E_{\mathrm{f}}(d,\boldsymbol{g})$.

It can be checked that $E_{\mathrm{f,\,lb}}(d,\boldsymbol{g})$ is the optimal objective function of the convex optimization problem shown in (39). By resorting to the KKT condition [33], the optimal objective function $E_{\mathrm{f,\,lb}}(d,\boldsymbol{g})$ can be derived as follows. Set $\lambda(\boldsymbol{g})$ to be the Lagrange multiplier associated with the constraint (39a), then the optimal solution of the convex optimization problem shown in (39) should satisfy the following equality

$$\frac{\sigma^2}{2w^2\tau^2 g_m}d_m^2=\lambda(\boldsymbol{g}),\forall m\in\{1,2,...,M\} \tag{40}$$

which indicates

$$d_m=\sqrt{\lambda(\boldsymbol{g})}\sqrt{\frac{2w^2\tau^2 g_m}{\sigma^2}},\forall m\in\{1,2,...,M\}. \tag{41}$$

Then substituting the expression of d_m for $m\in\{1,2,...,M\}$ in (41) into constraint (39a), we can derive a closed-form expression of $\lambda(\boldsymbol{g})$, which is given as

$$\lambda(\boldsymbol{g})=\frac{\sigma^2}{2w^2\tau^2}\left(\frac{d}{\sum_{m=1}^{M}\sqrt{g_m}}\right)^2. \tag{42}$$

Then substituting the $\lambda(\boldsymbol{g})$ expression in (41), we have

$$d_m=\frac{d\sqrt{g_m}}{\sum_{m=1}^{M}\sqrt{g_m}},\forall m\in\{1,2,...,M\}. \tag{43}$$

Hence $E_{\mathrm{f,\,lb}}(d,\boldsymbol{g})$ can be written as

$$E_{\mathrm{f,\,lb}}(d,\boldsymbol{g})=\sum_{m=1}^{M}\frac{\sigma^2}{6w^2\tau^2}\frac{d^3\sqrt{g_m}}{\left(\sum_{m=1}^{M}\sqrt{g_m}\right)^3} \tag{44}$$

which indicates that

$$\begin{aligned} E_{\mathrm{f,\,lb}}(d) &\triangleq\int E_{\mathrm{f,\,lb}}(d,\boldsymbol{g})f(\boldsymbol{g})d\boldsymbol{g}\\ &=d^3\tfrac{\sigma^2}{6w^2\tau^2}\int\frac{\sum_{m=1}^{M}\sqrt{g_m}}{\left(\sum_{m=1}^{M}\sqrt{g_m}\right)^3}f(\boldsymbol{g})d\boldsymbol{g}\\ &=d^3\tfrac{\sigma^2}{6w^2\tau^2}\int\left(\sum_{m=1}^{M}\sqrt{g_m}\right)^{-2}f(\boldsymbol{g})d\boldsymbol{g}. \end{aligned} \tag{45}$$

Therefore, the inverse function of $E_{\mathrm{f,\,lb}}(d)$ can be given as

$$\begin{aligned} &E_{\mathrm{f,\,lb}}^{-1}(E(n)\varepsilon)\\ &=\left(\frac{E(n)\varepsilon 6w^2\tau^2}{\sigma^2}\frac{1}{\int\left(\sum_{m=1}^{M}\sqrt{g_m}\right)^{-2}f(\boldsymbol{g})d\boldsymbol{g}}\right)^{\frac{1}{3}}\\ &\leq\left(\frac{E(n)\varepsilon 6w^2\tau^2}{\sigma^2}\frac{1}{\int\frac{1}{M^2h_{\mathrm{u}}}f(\boldsymbol{g})d\boldsymbol{g}}\right)^{\frac{1}{3}}\\ &=\left(\frac{E(n)\varepsilon 6w^2\tau^2M^2h_{\mathrm{u}}}{\sigma^2}\right)^{\frac{1}{3}} \end{aligned} \tag{46}$$

where h_{u} is the upper bound of the channel gain g_m since $f(g_m)=0$ for $g_m\geq h_{\mathrm{u}}$.

Since $E_{\text{f, lb}}(d, \boldsymbol{g})$ is a lower bound of the objective function of (35), we have

$$E_{\text{f}}(d, \boldsymbol{g}) \geq E_{\text{f, lb}}(d, \boldsymbol{g}), \tag{47}$$

and thereafter

$$E_{\text{f}}(d) \geq E_{\text{f, lb}}(d), \tag{48}$$

which can lead to

$$E_{\text{f}}^{-1}(E(n)\varepsilon) \leq E_{\text{f, lb}}^{-1}(E(n)\varepsilon) \tag{49}$$

by following the proof method in Lemma 6.

Combining (37), (49), and (46), we have

$$\begin{aligned} \lim_{M\to\infty} \frac{D_{\text{f}}(E(n),M)}{M} &\leq \lim_{M\to\infty} \frac{E_{\text{f, lb}}^{-1}(E(n)\varepsilon)}{M} \\ &\leq \lim_{M\to\infty} \left(\frac{E(n)\varepsilon 6 w^2 \tau^2 h_{\text{u}}}{M\sigma^2}\right)^{\frac{1}{3}} \\ &= 0. \end{aligned} \tag{50}$$

For $i = \text{p}$, define

$$\begin{aligned} &E_{\text{p}}(d, \boldsymbol{g}) \triangleq \\ &\min_{\{d_m | m\in\{1,2,\ldots,M\}\}} \quad \sum_{m=1}^{M} e(d_m, g_m) + E_{\text{L}}(d_{\text{L}}, M\tau) \\ &\qquad\qquad \text{s.t.} \quad \sum_{m=1}^{M} d_m + d_{\text{L}} = d, \\ &\qquad\qquad\qquad d_m \geq 0, \forall m \in \{1,2,...,M\}, \\ &\qquad\qquad\qquad d_{\text{L}} \geq 0. \end{aligned} \tag{51}$$

Here d_{L} means the amount of data nats that are locally calculated at the mobile device. Note that in the objective function shown in (51), the function $E_{\text{L}}(d_{\text{L}}, M\tau)$ is a monomial function of d_{L} with order 3, as shown in (9). Then by following the similar procedure for the discussion when $i = \text{f}$, it can be also derived that

$$\lim_{M\to\infty} \frac{D_{\text{p}}(E(n),M)}{M} = 0. \tag{52}$$

This completes the proof. ∎

Remark: Lemma 7 offers the following insight. For any stopping rule N, the solution $M = \infty$ cannot be optimal for Problem 3. In other words, we can perform one-dimensional search of M in finite steps to get the optimal M. Suppose the optimal M is searched between 1 and $M_{\max}$. Then the computational complexity of solving Problem 3 is $O(M_{\max})$.

VI. Numerical Results

Similar to [10], [18], we use the following system parameters: the number of CPU cycles for computing one data nat $c_0 = 40$, the fixed coefficient characterizing the mobile device's CPU $k = 10^{-28}$, the length of one fading block $\tau = 1$ms, the energy conversion efficiency of the energy harvester $\eta = 0.3$, the maximal energy capacity of the energy harvester's battery $C = 20$J, the bandwidth of one channel $w = 1$MHz, the noise power spectrum density $\sigma^2 = -140$ dBmW/Hz, the transmit power $P_E = 0.5$ W, the efficiency of the amplifier at the transmitter of the mobile device $\varepsilon = 1$. The channel between the BS and the mobile device experiences Rayleigh fading. Thus, channel gain is exponentially distributed. The mean of channel gain, denoted as θ, is set as 10^{-6}, which corresponds to the attenuation at a distance of 47.7m with a carrier frequency 500MHz in free space. To save the computation complexity, the number of fading blocks for data offloading M would be searched between the interval $[0, 30]$. For the ease of presentation, the average processed data amount in unit time, i.e., the objective function of Problem 1 would be written as "Average processing rate" in this section.

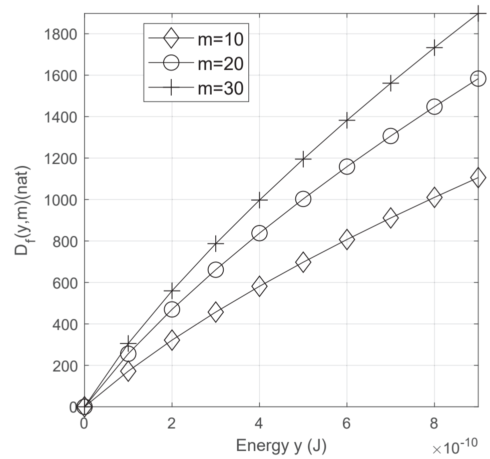

Fig. 3: Verification of Lemma 1.

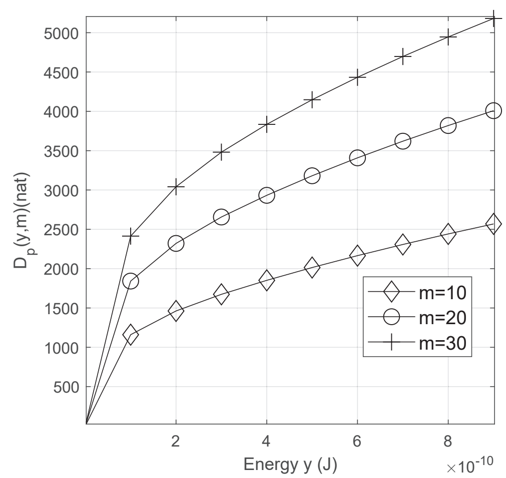

Fig. 4: Verification of Lemma 2.

Fig. 3 and Fig. 4 plot the function of $D_{\text{f}}(y, m)$ and $D_{\text{p}}(y, m)$ versus y for $m = 10$, $m = 20$ and $m = 30$, respectively. It can be seen that both the function $D_{\text{f}}(y, m)$ and $D_{\text{p}}(y, m)$ are increasing and concave function with y for given m. These results verify the claims that are given in Lemma 1 and Lemma 2.

Fig. 5 and Fig. 6 plot the function of $J_m(d)$ and $\Lambda_m(d)$ versus m when $d = 80$ nat, $d = 800$ nat, and $d = 1600$ nat, respectively. It can be observed that as m increases, both function $J_m(d)$ and function $\Lambda_m(d)$ go down. These results verify the claims in Lemma 4 and Lemma 5.

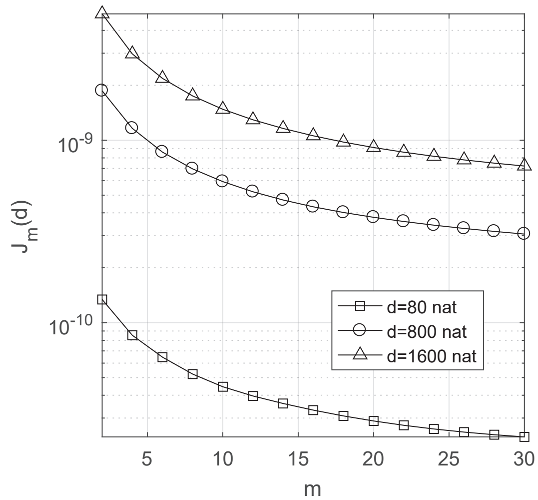

Fig. 5: Verification of Lemma 4.

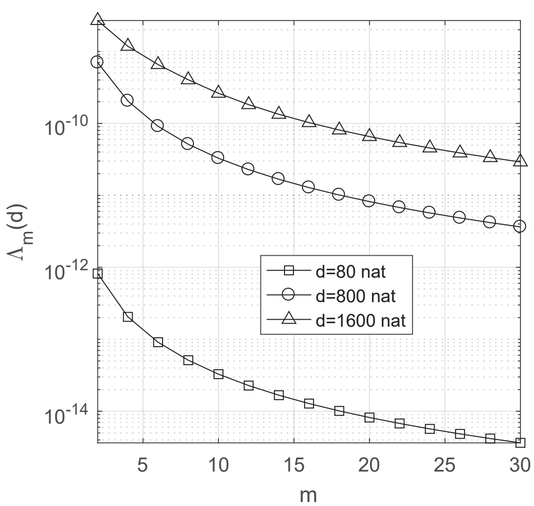

Fig. 6: Verification of Lemma 5.

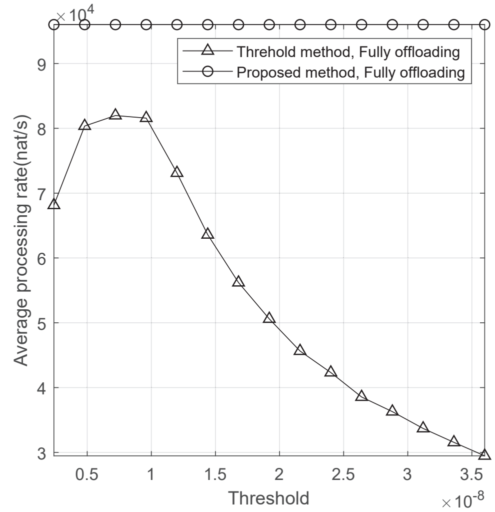

Fig. 7: Comparison with the threshold policy under fully offloading mode.

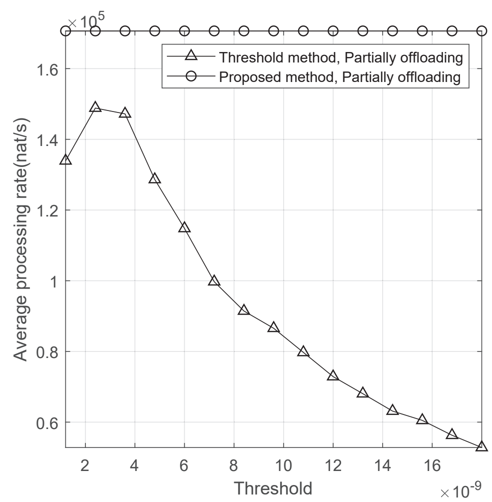

Fig. 8: Comparison with the threshold policy under partially offloading mode.

In Fig. 7 and Fig. 8, our proposed method is compared with a threshold strategy, which compares the total harvested energy $\sum_{n'=1}^{n} P_E \eta h_{n'} \tau$ with a fixed-value threshold and will stop at the nth fading block if $\sum_{n'=1}^{n} P_E \eta h_{n'} \tau$ is larger than the selected threshold. Various threshold values are listed in Fig. 7 and Fig. 8. The results show that our method outperforms the threshold policy, which verifies the advantage of our proposed method.

In Fig. 9, the average processing rate versus transmit power P_E of the BS is investigated under fully offloading mode and partially offloading mode. It can be observed that the optimal solution under partially offloading mode always outperforms the one under fully offloading mode. This can be explained by the fact that the fully offloading mode is only a feasible solution of partially offloading mode, which will be no better than the optimal solution under partially offloading mode for sure. As a comparison, two methods in [17] are realized. For the first method, the harvested energy will be fully utilized at local (i.e., offloading is not performed). This method is called "Local computing" here. For the second method, one round of charging and fully offloading is performed in every fading block, which means that in a fading block, the mobile device first harvests energy and then offloads data for computing. This method is called "One round in one block" here. To maximize the processing rate under the setup of the second method in [17], the optimal charging time is found to be $\frac{\tau}{3}$. From Fig. 9, it can be observed that as the transmit power P_E increases, the average processing rate grows in all methods. This is because the increase of P_E contributes to higher harvested energy and higher throughput for data offloading in unit time. In addition, both partially offloading mode and fully offloading

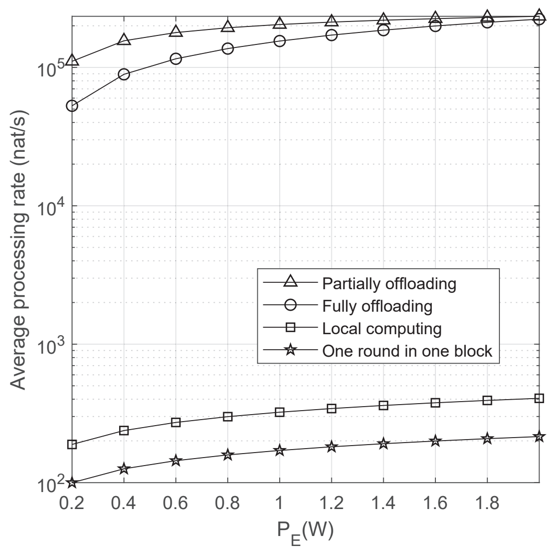

Fig. 9: Average processing rate versus P_E.

mode outperform the local computing method and one round in one block method, which demonstrates the advantage of our proposed method.

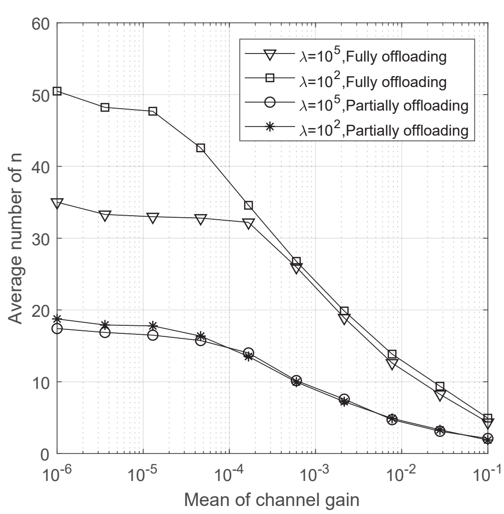

Fig. 10: Average stopping time versus mean channel gain.

In Fig. 10, the average number of EH fading blocks (at stopping) is plotted versus the mean of channel gain under both partially offloading mode and fully offloading mode with different λ values. It can be seen that Algorithm 1 usually stops within 50 steps. It can be also seen that as the mean of channel gain increases, the average number of EH fading blocks (at stopping) trends to decrease. This is because a better channel leads to a higher energy arrival rate, which permits the mobile device to collect enough energy earlier.

VII. Conclusion

In this paper, we investigate a wireless-powered MEC system, in which a target mobile device first harvests energy from radio frequency signals of a BS and then offloads the data to be processed to the BS. The whole process may span over multiple fading blocks. For data offloading, both the fully offloading and partially offloading are considered. The expected data processing rate is maximized. To achieve the goal, both the stopping rule for energy harvesting and the number of fading blocks for offloading are optimized. To solve the associated optimization problem, we decompose it into two levels. In the lower level, with the number of fading blocks for offloading fixed, the optimal stoping rule for energy harvesting is derived. In the upper level, the number of fading blocks for offloading is optimized. This research can provide helpful insights for the implementation of wireless-powered mobile devices in IoT networks.

In our research, when the partially offloading mode is used, the mobile device's local computing is performed only in offloading fading blocks (i.e., after energy harvesting process is finished and the available energy amount is known). Based on (9), it can be seen that the energy used for local computing is reduced if the local computing time duration increases. Thus, the system performance can be further improved if the mobile device can also perform its local computing in EH fading blocks. Then at each EH fading block, the mobile device needs to decide how much energy is used in the current fading block for local computing and how much energy is reserved for future use (i.e., for offloading and local computing during the offloading fading blocks). As the mobile device does not know energy arrival rates in subsequent EH fading blocks, it is challenging for the mobile device to make an optimal decision, which deserves further research efforts.

Appendix A
Proof of Lemma 1

First, we prove that $J_m(d)$ is an increasing function by induction method. It can be easily checked that $J_1(d)$ and $Q_1(d,x)$ are increasing function with respect to d. Suppose both $J_{m-1}(d)$ and $Q_{m-1}(d,x)$ are increasing with respect to d. Denote $d_m^*(d,x)$ as the optimal solution of d' in the minimization problem in (6) when there are m fading blocks left and d data nats to be transmitted for data offloading, and $g_m = x$. Consider two values of d: $d^\dagger > d^\ddagger$.

When $0 \le d_m^*(d^\dagger, x) \le d^\ddagger$, we have

$$\begin{aligned} Q_m(d^\dagger, x) \quad &= e(d_m^*(d^\dagger,x),x) + J_{m-1}\left(d^\dagger - d_m^*(d^\dagger,x)\right) \\ &> e(d_m^*(d^\dagger,x),x) + J_{m-1}\left(d^\ddagger - d_m^*(d^\dagger,x)\right) \\ &\ge e(d_m^*(d^\ddagger,x),x) + J_{m-1}\left(d^\ddagger - d_m^*(d^\ddagger,x)\right) \\ &= Q_m(d^\ddagger, x). \end{aligned} \tag{53}$$

When $d^\ddagger < d_m^*(d^\dagger, x) \le d^\dagger$, we have

$$\begin{aligned} Q_m(d^\ddagger, x) \quad &= e(d_m^*(d^\ddagger,x),x) + J_{m-1}\left(d^\ddagger - d_m^*(d^\ddagger,x)\right) \\ &\le e(d^\ddagger, x) + J_{m-1}\left(d^\ddagger - d^\ddagger\right) \\ &= e(d^\ddagger, x). \end{aligned} \tag{54}$$

Then according to (54), we have

$$\begin{aligned} Q_m(d^\dagger,x) &= e(d_m^*(d^\dagger,x),x) + J_{m-1}\left(d^\dagger - d_m^*(d^\dagger,x)\right) \\ &\geq e(d_m^*(d^\dagger,x),x) \\ &\quad + J_{m-1}\left(d_m^*(d^\dagger,x) - d_m^*(d^\dagger,x)\right) \\ &= e(d_m^*(d^\dagger,x),x) \\ &> e(d^\ddagger,x) \\ &\geq Q_m(d^\ddagger,x). \end{aligned} \tag{55}$$

Thus, it can be concluded that $Q_m(d,x)$ is an increasing function with respect to d. Based on (5), $J_m(d)$ is also an increasing function with respect to d.

Finally, we look into $D_\mathrm{f}(y,m)$. Since $D_\mathrm{f}(y,m) = J_m^{-1}(y\cdot\varepsilon)$, we have

$$\begin{aligned} D_\mathrm{f}'(y,m) &= \varepsilon \frac{\mathrm{d}J_m^{-1}(y\cdot\varepsilon)}{\mathrm{d}(y\varepsilon)} \\ &= \frac{\varepsilon}{J_m'(J_m^{-1}(y\varepsilon))} \\ &= \frac{\varepsilon}{J_m'(D_\mathrm{f}(y,m))} \\ &> 0 \end{aligned} \tag{56}$$

where $D_\mathrm{f}'(y,m)$ and $J_m'(\cdot)$ are the first-order derivative of $D_\mathrm{f}(y,m)$ (with respect to y) and $J_m(\cdot)$, respectively, and the inequality holds since the function $J_m(\cdot)$ is increasing and thus its derivative is always positive. Thus, $D_\mathrm{f}(y,m)$ is an increasing function of y.

In addition, since $J_m(\cdot)$ is a convex function (which can be proved by using an induction method, with the aid of [34, Theorem 5.4]), $J_m'(\cdot)$ is an increasing function. Recalling that $D_\mathrm{f}'(y,m) = \frac{\varepsilon}{J_m'(D_\mathrm{f}(y,m))}$, it can be derived that $D_\mathrm{f}'(y,m)$ is a decreasing function of y, which proves the concavity of $D_\mathrm{f}(y,m)$ with y.

This completes the proof.

Appendix B
Proof of Lemma 2

By following the proof method in Lemma 1, to prove the increasing monotonicity and concavity of $D_\mathrm{p}(y,m)$, we only need to prove that $\Lambda_m(x)$ is increasing and convex with x.

For the increasing monotonicity, looking into the Problem in (10). Suppose $D^\dagger < D^\ddagger$. Assume the optimal solution of the Problem in (10) when $D = D^\dagger$ and $D = D^\ddagger$ are $D_\mathrm{E}^\dagger$ and $D_\mathrm{E}^\ddagger$, respectively. When $0 \leq D_\mathrm{E}^\ddagger \leq D^\dagger$, we have

$$\begin{aligned} \Lambda_m(D^\dagger) &= E_\mathrm{L}(D^\dagger - D_\mathrm{E}^\dagger, m\tau) + J_m(D_\mathrm{E}^\dagger) \\ &\leq E_\mathrm{L}(D^\dagger - D_\mathrm{E}^\ddagger, m\tau) + J_m(D_\mathrm{E}^\ddagger) \\ &< E_\mathrm{L}(D^\ddagger - D_\mathrm{E}^\ddagger, m\tau) + J_m(D_\mathrm{E}^\ddagger) \\ &= \Lambda_m(D^\ddagger). \end{aligned} \tag{57}$$

When $D^\dagger < D_\mathrm{E}^\ddagger \leq D^\ddagger$, we have

$$\begin{aligned} \Lambda_m(D^\dagger) &= E_\mathrm{L}(D^\dagger - D_\mathrm{E}^\dagger, m\tau) + J_m(D_\mathrm{E}^\dagger) \\ &\leq E_\mathrm{L}(D^\dagger - D^\dagger, m\tau) + J_m(D^\dagger) \\ &= J_m(D^\dagger), \end{aligned} \tag{58}$$

and

$$\begin{aligned} \Lambda_m(D^\ddagger) &= E_\mathrm{L}(D^\ddagger - D_\mathrm{E}^\ddagger, m\tau) + J_m(D_\mathrm{E}^\ddagger) \\ &\geq E_\mathrm{L}(D_\mathrm{E}^\ddagger - D_\mathrm{E}^\ddagger, m\tau) + J_m(D_\mathrm{E}^\ddagger) \\ &= J_m(D_\mathrm{E}^\ddagger) \\ &> J_m(D^\dagger) \\ &\geq \Lambda_m(D^\dagger) \end{aligned} \tag{59}$$

in which the last inequality comes from (58). Thus, the increasing monotonicity of $\Lambda_m(D)$ with D has been proved.

For the convexity, consider two different values $x^\dagger$ and $x^\ddagger$. Define $D_\mathrm{E}^\dagger$ and $D_\mathrm{E}^\ddagger$ as the optimal solutions of the Problem in (10) when $D = x^\dagger$ and $D = x^\ddagger$, respectively. For $\forall\alpha \in [0,1]$, denote D_E^* as the optimal solution of the Problem in (10) when $D = \alpha x^\dagger + (1-\alpha)x^\ddagger$. Then we have

$$\begin{aligned} & \alpha\Lambda_m(x^\dagger) + (1-\alpha)\,\Lambda_m(x^\ddagger) \\ = \;& \alpha E_\mathrm{L}(x^\dagger - D_\mathrm{E}^\dagger, m\tau) + (1-\alpha)E_\mathrm{L}(x^\ddagger - D_\mathrm{E}^\ddagger, m\tau) \\ & + \alpha J_m(D_\mathrm{E}^\dagger) + (1-\alpha)J_m(D_\mathrm{E}^\ddagger) \\ \overset{(a)}{\geq} \;& E_\mathrm{L}\left(\left(\alpha x^\dagger + (1-\alpha)x^\ddagger\right) - \left(\alpha D_\mathrm{E}^\dagger + (1-\alpha)D_\mathrm{E}^\ddagger\right), m\tau\right) \\ & + J_m\left(\left(\alpha D_\mathrm{E}^\dagger + (1-\alpha)D_\mathrm{E}^\ddagger\right)\right) \\ \overset{(b)}{\geq} \;& E_\mathrm{L}\left(\left(\alpha x^\dagger + (1-\alpha)x^\ddagger\right) - D_\mathrm{E}^*, m\tau\right) + J_m\left(D_\mathrm{E}^*\right) \\ = \;& \Lambda_m(\alpha x^\dagger + (1-\alpha)x^\ddagger) \end{aligned}$$

where (a) holds since both the function $E_\mathrm{L}(\cdot)$ and the function $J_m(\cdot)$ are convex, and (b) is due to the fact that $\left(\alpha D_\mathrm{E}^\dagger + (1-\alpha)D_\mathrm{E}^\ddagger\right)$ is a feasible solution of the Problem in (10) when $D = \left(\alpha x^\dagger + (1-\alpha)x^\ddagger\right)$ and will have no better performance compared with D_E^* (recalling that D_E^* is the optimal solution of the Problem in (10) when $D = \alpha x^\dagger + (1-\alpha)x^\ddagger$).

This completes the proof.

Appendix C
Proof of Lemma 4

Recalling that $d_m^*(d,x)$ is the optimal solution of d' in the minimization problem in (6) when there are m fading blocks left and d data nats to be transmitted for data offloading, and $g_m = x$. There is

$$\begin{aligned} & Q_m(d,x) \\ = \;& e(d_m^*(d,x),x) + \int_0^\infty Q_{m-1}\left(d - d_m^*(d,x),x'\right)f(x')dx' \\ \leq \;& e(0,x) + \int_0^\infty Q_{m-1}(d-0,x')f(x')dx' \\ = \;& J_{m-1}(d), \end{aligned} \tag{60}$$

in which x represents a value of g_m, and x' represents a value of g_{m-1}. Hence we have

$$\begin{aligned} J_m(d) &= \int_0^\infty Q_m(d,x)f(x)dx \\ &\leq \int_0^\infty J_{m-1}(d)f(x)dx \\ &= J_{m-1}(d), \end{aligned} \tag{61}$$

in which x represents a value of g_m.

This completes the proof.

Appendix D
Proof of Lemma 5

Suppose $d_\mathrm{E}^*(d,m)$ is the optimal solution of the Problem in (10) when the amount of data to be processed is d nats (i.e., $D = d$) and there are m fading blocks left for data offloading (i.e., $M = m$). For $m^\dagger < m^\ddagger$, we have

$$\begin{aligned} \Lambda_{m^\dagger}(d) &= E_\mathrm{L}(d - d_\mathrm{E}^*(d,m^\dagger), m^\dagger\tau) + J_{m^\dagger}(d_\mathrm{E}^*(d,m^\dagger)) \\ &\overset{(a)}{>} E_\mathrm{L}(d - d_\mathrm{E}^*(d,m^\dagger), m^\ddagger\tau) + J_{m^\ddagger}(d_\mathrm{E}^*(d,m^\dagger)) \\ &\overset{(b)}{\geq} E_\mathrm{L}(d - d_\mathrm{E}^*(d,m^\ddagger), m^\ddagger\tau) + J_{m^\ddagger}(d_\mathrm{E}^*(d,m^\ddagger)) \\ &= \Lambda_{m^\ddagger}(d) \end{aligned} \tag{62}$$

where (a) comes from Lemma 4 and (b) is due to the fact that both $d_{\mathrm{E}}^{*}(d, m^{\dagger})$ and $d_{\mathrm{E}}^{*}(d, m^{\ddagger})$ lie in the interval $[0, d]$ and no solution lying in $[0, d]$ can achieve better performance than $d_{\mathrm{E}}^{*}(d, m^{\ddagger})$ in the Problem in (10) with $M = m^{\ddagger}$ and $D = d$.

This completes the proof.

Appendix E
Proof of Lemma 6

It is evident that function $\mathbb{E}[\tau_{N,M}]$ is monotonic increasing with M for given N.

Next the monotonicity of function $\mathbb{E}[D_{\mathrm{f}}(E(N), M)]$ with M is proved. Suppose $m^{\dagger} < m^{\ddagger}$, for $N = n$, define $d^{\dagger} = D_{\mathrm{f}}(E(n), m^{\dagger})$ and $d^{\ddagger} = D_{\mathrm{f}}(E(n), m^{\ddagger})$. Then we have

$$\varepsilon E(n) = J_{m^{\dagger}}(d^{\dagger}) = J_{m^{\ddagger}}(d^{\ddagger}). \tag{63}$$

Combining the fact that $J_{m^{\dagger}}(d) > J_{m^{\ddagger}}(d)$ according to Lemma 4, it can be inferred that

$$d^{\dagger} < d^{\ddagger}. \tag{64}$$

Thus, for $m^{\dagger} < m^{\ddagger}$, $D_{\mathrm{f}}(E(n), m^{\dagger}) < D_{\mathrm{f}}(E(n), m^{\ddagger})$, which further indicates that $\mathbb{E}[D_{\mathrm{f}}(E(n), m^{\dagger})] < \mathbb{E}[D_{\mathrm{f}}(E(n), m^{\ddagger})]$.

At last, by combing the result in Lemma 5 and following the proof for the monotonicity of function $\mathbb{E}[D_{\mathrm{f}}(E(N), M)]$ with M, the monotonicity of function $\mathbb{E}[D_{\mathrm{p}}(E(N), M)]$ with M can be proved.

This completes the proof.

References

[1] A. H. H. Ngu, M. Gutierrez, V. Metsis, S Nepal, and Q. Z. Sheng, "IoT middleware: A survey on issues and enabling technologies," *IEEE Internet Things J.*, vol. 4, no. 1, pp. 1–20, Feb. 2017.

[2] X. Gao, P. Wang, D. Niyato, K. Yang, and J. An, "Auction-based time scheduling for backscatter-aided RF-powered cognitive radio networks," *IEEE Trans. Wireless Commun.*, vol. 18, no. 3, pp. 1684–1697, Mar. 2019.

[3] D. Lin, Y. Tang, Y. Yao, and A. V. Vasilakos, "User-priority-based power control over the D2D assisted Internet of vehicles for mobile health," *IEEE Internet Things J.*, vol. 4, no. 3, pp. 824–831, June 2017.

[4] J. Yu, W. Gong, J. Liu, L. Chen, K. Wang, and R. Zhang, "Missing tag identification in COTS RFID systems: Bridging the gap between theory and practice," *IEEE Trans. Mobile Comput.*, vol. 19, no. 1, pp. 130–141, Jan. 2020.

[5] M. Swan, "Sensor mania! The Internet of Things, wearable computing, objective metrics, and the qualified 2.0," *J. Sensor Actuator Netw.*, vol. 1, no. 3, pp. 217–253, Nov. 2012.

[6] F. Liu, P. Shu, and J. C. S. Lui, "AppATP: An energy conserving adaptive mobile-cloud transmission protocol," *IEEE Trans. Comput.*, vol. 64, no. 11, pp. 3051–3063, Nov. 2015.

[7] F. Liu, P. Shu, H. Jin, and L. Ding, "Gearing resource-poor mobile devices with powerful clouds: Architectures, challenges, and applications," *IEEE Wireless Commun.*, vol. 20, no. 3, pp. 14–22, June 2013.

[8] T. X. Tran, A. Hajisami, P. Pandey, and D. Pompili, "Collaborative mobile edge computing in 5G networks: New paradigm, scenarios, and challenges," *IEEE Commun. Mag.*, vol. 55, no. 4, pp. 54–61, Apr. 2017.

[9] A. C. Baktir, A. Ozgovde, and C. Ersoy, "How can edge computing benefit from software-defined networking: A survey, use cases and future directions," *IEEE Commun. Surveys Tuts.*, vol. 19, no. 4, pp. 2359–2391, 4th Quart., 2017.

[10] C. You, K. Huang, H. Chae, and B. H. Kim, "Energy-efficient resource allocation for mobile-edge computation offloading," *IEEE Trans. Wireless Commun.*, vol. 16, no. 3, pp. 1397–1411, Mar. 2017.

[11] C. You, Y. Zeng, R. Zhang, and K. Huang, "Asynchronous mobile-edge computation offloading: Energy-efficient resource management," *IEEE Trans. Wireless Commun.*, vol. 17, no. 11, pp. 7590–7605, Nov. 2018.

[12] J. An, K. Yang, J. Wu, N. Ye, S. Guo, and Z. Liao, "Achieving sustainable ultra-dense heterogeneous networks for 5G," *IEEE Commun. Mag.*, vol. 55, no. 12, pp. 84–90, Dec. 2017.

[13] T. K. Rodrigues, K. Suto, H. Nishiyama, J. Liu, and N. Kato, "Machine learning meets computation and communication control in evolving edge and cloud: Challenges and future perspective," *IEEE Commun. Surveys Tuts.*, vol. 22, no. 1, pp. 38–67, 1st Quart., 2020.

[14] S. Bi, Y. Zeng, and R. Zhang, "Wireless powered communication networks: An overview," *IEEE Wireless Commun.*, vol. 23, no. 2, pp. 10–18, Apr. 2016.

[15] Y. Mao, C. You, J. Zhang, K. Huang, and K. B. Letaief, "A survey on mobile edge computing: The communication perspective," *IEEE Commun. Surveys Tuts.*, vol. 19, no. 4, pp. 2322–2358, 4th Quart., 2017.

[16] X. Hu, K.-K. Wong, and K. Yang, "Wireless powered cooperation-assisted mobile edge computing," *IEEE Trans. Wireless Commun.*, vol. 17, no. 4, pp. 2375–2388, Apr. 2018.

[17] C. You, K. Huang, and H. Chae, "Energy efficient mobile cloud computing powered by wireless energy transfer," *IEEE J. Sel. Areas Commun.*, vol. 34, no. 5, pp. 1757–1771, May 2016.

[18] Y. Wang, M. Sheng, X. Wang, L. Wang, and J. Li, "Mobile-edge computing: Partial computation offloading using dynamic voltage scaling," *IEEE Trans. Commun.*, vol. 64, no. 10, pp. 4268–4282, Oct. 2016.

[19] C. You and K. Huang, "Exploiting non-causal CPU-state information for energy-efficient mobile cooperative computing," *IEEE Trans. Wireless Commun.*, vol. 17, no. 6, pp. 4104–4117, June 2018.

[20] O. Muñoz, A. Pascual-Iserte, and J. Vidal, "Optimization of radio and computational resources for energy efficiency in latency-constrained application offloading," *IEEE Trans. Veh. Technol.*, vol. 64, no. 10, pp.4738–4755, Oct. 2015.

[21] D. Tse and P. Viswanath, *Fundamentals of Wireless Communication*. Cambridge, U.K.:: Cambridge Univ. Press, 2005.

[22] J. Zhao, R. S. Allison, M. Vinnikov, and S. Jennings, "Estimating the motion-to-photon latency in head mounted displays," in *Proc. 5th IEEE Virtual Reality*, Mar. 2017, pp. 313–314.

[23] H. Li, K. Ota, and M. Dong, "Learning IoT in edge: Deep learning for the Internet of things with edge computing," *IEEE Netw.*, vol. 32, no. 1, pp. 96–101, Jan.-Feb. 2018.

[24] F. Tang, Z. M. Fadlulah, B. Mao, and N. Kato, "An intelligent traffic load prediction-based adaptive channel assignment algorithm in SDN-IoT: A deep learning approach," *IEEE Internet Things J.*, vol. 5, no. 6, pp. 5141–5154, Dec. 2018.

[25] K. Miyanabe, T. G. Rodrigues, Y. Lee, H. Nishiyama, and N. Kato, "An Internet of things traffic-based power sving scheme in cloud-radio access network," *IEEE Internet Things J.*, vol. 6, no. 2, pp. 3087–3096, Apr. 2019.

[26] F. Samie, V. Tsoutsouras, L. Bauer, S. Xydis, D. Soudris, and J. Henkel, "Computation offloading and resource allocation for low-power IoT edge devices," in *Proc. IEEE 3rd World Forum Internet Things (WF-IoT)*, Dec. 2016, pp. 7–12.

[27] T. G. Rodrigues, K. Suto, H. Nishiyama, and N. Kato, "Cloudlets activation scheme for scalable mobile edge computing with transmission power control and virtual machine migration," *IEEE Trans. Comput.*, vol. 67, no. 9, pp. 1287–1300, Sep. 2018.

[28] T. K. Rodrigues, K. Suto, and N. Kato, "Edge cloud server deployment with transmission power control through machine learning for 6G Internet of things," *IEEE Trans. Emerging Topics in Computing*, to be published, DOI: 10.1109/TETC.2019.2963091.

[29] W. Zhang, Y. Wen, K. Guan, D. Kilper, H. Luo, and D. O. Wu, "Energy-optimal mobile cloud computing under stochastic wireless channel," *IEEE Trans. Wireless Commn.*, vol. 12, no. 9, pp. 4569–4581, Sep. 2013.

[30] R. Fan, F. Li, S. Jin, G. Wang, H. Jiang, and S. Wu, "Energy-efficient mobile-edge computation offloading over multiple fading blocks," in *Proc. IEEE GLOBECOM*, Dec. 2019, pp. 1–6.

[31] D. P. Bertsekas, *Dynamic Programming and Optimal Control*. Belmont, MA, USA: Athena Scientific, 2017.

[32] T. Ferguson, *Optimal stopping and applications*, Mathematics Dept., UCLA. [Online]. Available: http://www.math.ucla.edu/~tom/Stopping/Contents.html.

[33] S. P. Boyd and L. Vandenberghe, *Convex Optimization.* Cambridge, U.K.: Cambridge Univ. Press, 2004.

[34] R. T. Rockafellar, *Convex Analysis*. Princeton, NJ, USA: Princeton Univ. Press, 1970.

Qi Gu received the B.E. degree from Civil Aviation University of China, Tianjin, China, in 2013, and the M.S. and Ph.D. degree from Beijing Jiaotong University, Beijing, China, in 2015 and 2020, respectively. Her research interests include energy harvesting and edge computing.

Yiheng Jian received the B.E. degree from Beijing Institution of Technology, Beijing, China, in 2020. His research interests include software engineering and edge computing.

Gongpu Wang (Member, IEEE) received the B.Eng. degree in communication engineering from Anhui University, Hefei, China, in 2001 and the M.Sc. degree from Beijing University of Posts and Telecommunications (BUPT), China, in 2004, and the Ph.D. degree from the University of Alberta, Edmonton, Alberta, Canada, in 2011. From 2004 to 2007, he was an Assistant Professor at the School of Network Education, BUPT. After Ph.D. graduation, he joined the School of Computer and Information Technology, Beijing Jiaotong University (BJTU), China, where he is currently a Professor. His research interests include wireless communication theory and signal processing technologies.

Rongfei Fan (Member, IEEE) received the B.E. degree in communication engineering from Harbin Institute of Technology, Harbin, China, in 2007, and the Ph.D. degree in electrical engineering from the University of Alberta, Edmonton, Alberta, Canada, in 2012. Since 2013, he has been a faculty member at the Beijing Institute of Technology, Beijing, China, where he is currently an Associate Professor in the School of Information and Electronics. His research interests include edge computing, resource allocation in wireless networks, and statistical signal processing.

Hai Jiang (Senior Member, IEEE) received the B.Sc. and M.Sc. degrees in electronics engineering from Peking University, Beijing, China, in 1995 and 1998, respectively, and the Ph.D. degree in electrical engineering from the University of Waterloo, Waterloo, ON, Canada, in 2006. Since 2007, he has been a Faculty Member with the University of Alberta, Edmonton, AB, Canada, where he is currently a Professor with the Department of Electrical and Computer Engineering. His research interests include radio resource management, cognitive radio networking, and cooperative communications.

Zhangdui Zhong (Senior Member, IEEE) received the B.E. and M.S. degrees from Beijing Jiaotong University (BJTU), Beijing, China, in 1983 and 1988, respectively. He is currently a Professor with BJTU, where he is also a Chief Scientist of the State Key Laboratory of Rail Traffic Control and Safety. He is also a Director of the Innovative Research Team of the Ministry of Education, Beijing, and a Chief Scientist of the Ministry of Railways, Beijing. His research interests include wireless communications for railways, control theory and techniques for railways, and GSM-R systems. His research has been widely used in railway engineering, such as at the Qinghai-Xizang railway, the Datong-Qinhuangdao Heavy Haul railway, and many high-speed railway lines in China. He is an Executive Council member of the Radio Association of China, Beijing, and a Deputy Director of Radio Association, Beijing. He has authored or co-authored seven books, five invention patents, and over 200 scientific research papers in his research area. He received the MaoYiSheng Scientific Award of China, the ZhanTianYou Railway Honorary Award of China, and the Top 10 Science/Technology Achievements Award of Chinese Universities.